THE JOURNAL OF PHYSICAL CHEMISTRY C

Article

pubs.acs.org/JPCC

Physisorption Controls the Conformation and Density of States of an Adsorbed Porphyrin

S. P. Jarvis,*[,†] S. Taylor,[†] J. D. Baran,[‡] D. Thompson,[§] A. Saywell,[†,#] B. Mangham,[∥] N. R. Champness,[∥] J. A. Larsson,[⊥] and P. Moriarty[†]

[†]School of Physics & Astronomy, University of Nottingham, Nottingham NG7 2RD, U.K.

[‡]Department of Chemistry, University of Bath, Claverton Down, Bath BA2 7AY, U.K.

[§]Materials and Surface Science Institute and Department of Physics and Energy, University of Limerick, Castletroy, Ireland

[∥]School of Chemistry, University of Nottingham, Nottingham NG7 2RD, U.K.

[⊥]Applied Physics, Division of Materials Science, Department of Engineering Sciences and Mathematics, Luleå University of Technology, SE-971 87 Luleå, Sweden

[#]Fritz Haber Institute of the Max-Planck Society, 14195 Berlin, Germany

Supporting Information

ABSTRACT: Conformational changes caused by adsorption can dramatically affect a molecule's properties. Despite extensive study, however, the exact mechanisms underpinning conformational switching are often unclear. Here we show that the conformation of a prototypical flexible molecule, the free-base tetra(4-bromophenyl) porphyrin, adsorbed on Cu(111), depends critically on its precise adsorption site and that, remarkably, large conformational changes are dominated by van der Waals interactions between the molecule and the substrate surface. A combination of scanning probe microscopy, single-molecule manipulation, DFT with dispersion density functional theory, and molecular dynamics simulations show that van der Waals forces drive significant distortions of the molecular architecture so that the porphyrin can adopt one of two low-energy conformations. We find that adsorption driven by van der Waals forces alone is capable of causing large shifts in the molecular density of states, despite the apparent absence of chemical interactions. These findings highlight the essential role that van der Waals forces play in determining key molecular properties.

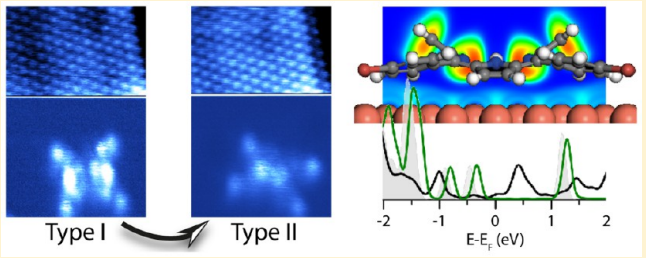

INTRODUCTION

The conformation of a molecule generally underpins its physicochemical properties and its ability to respond to changes in its environment. Structural flexibility is a key prerequisite for conformational variation leading to a critical interdependence between molecular form and function. Porphyrin molecules, and related molecules that exploit a tetrapyrrole motif, can couple conformational and functional change in a number of ways, including via distortion of the core macrocycle.[1−3] This is widely exploited in biological systems, where tetrapyrrole-based molecular frameworks are the basis of hemes[4] (including hemoglobin and other hemeproteins such as cytochromes) and corrin, the core of vitamin B_{12}.[5] The closely related class of chlorins, which, like the porphyrins, comprise a heterocyclic aromatic ring, consist of three pyrroles and one pyrroline and form, for example, the functional unit of chlorophyll.[6]

While the liquid phase and *in vitro* biophysics and biochemistry of porphyrins have been investigated in considerable detail, the potential of (metallo)porphyrins as elements of prototypical molecular electronics systems has led to significant growth in studies of their interaction with solid surfaces including, in particular, those of the so-called coinage metals: Au, Ag, and Cu. The gas-phase flexibility of the porphyrin macrocycle and any associated ligands tends to be preserved at metal surfaces such that a number of distinct conformers are observed. Copper surfaces—including, in particular, the Cu(111) surface which is the adsorption "platform" for the studies of conformational variations described below—have been widely used as substrates for porphyrin deposition.

The amount of literature surrounding porphyrin adsorption on noble metal surfaces is vast.[7] Reports range from studies involving metalated and nonmetalated cores to molecules possessing ligands such as tetraphenyl porphyrins each adsorbed on various metal surfaces such as Cu, Ag, and Au, the variety of which make comparisons between each individual system challenging. As summarized below, in the current understanding of tetraphenyl porphyrin (TPP) adsorption on Cu(111) there are two primary explanations for the observed

Received: August 27, 2015
Revised: November 19, 2015

DOI: 10.1021/acs.jpcc.5b08350
J. Phys. Chem. C XXXX, XXX, XXX−XXX

adsorption: (i) that adsorption is dominated by chemical interactions between the iminic nitrogens of the core and the metal substrate and (ii) that adsorption is instead dominated by attractive van der Waals (vdW) interactions between the phenyl legs and porphyrin core of the molecule with the surface. It should be noted, of course, that the two need not be mutually exclusive.

Claims of a chemical bonding interaction between the iminic nitrogen atoms in the porphyrin core and the underlying Cu(111) surface have been put forward in a number of papers.[8−11] In particular, the photoemission and X-ray absorption spectroscopy data of Doyle et al.[10] on tetra(4-bromophenyl)-porphyrins (Br_4TPP) were interpreted in terms of the formation of an intermediate Br_4TPP−Cu complex involving Cu-iminic N bonding following room-temperature adsorption. This was in analogy with the complete metalation of the molecule occurring following annealing at much higher temperatures (∼420 K). Since this publication, however, it has been noted that room-temperature deposition of Br_4TPP would lead to dehalogenation of the molecule, significantly affecting its properties.[12] Shortly following the publication of Doyle et al.'s results, photoelectron spectroscopy data for a submonolayer coverage of the 2H-TPP molecule on Cu(111) were interpreted in terms of the formation of strong localized bonds between the iminic nitrogen atoms and the copper surface.[8] Diller et al.[11] also found evidence of the interaction of the iminic nitrogen atoms of the 2H-TPP molecule with the underlying Cu(111) substrate, with the N lone pairs pointing toward the copper surface. Their photoemission data strongly suggested that photoelectron diffraction was responsible for variations in the intensity of the iminic and pyrrolic components of the N 1s core-level peak. This points to a well-defined adsorption site driven by the N−Cu interaction as coherence in the binding sites is a prerequisite for photoelectron diffraction. We note, however, that Diller et al. make the important point that binding energy shifts observed in photoemission spectra need not necessarily arise from a strong chemical interaction and can be due to screening of the photoinduced core hole (i.e., a final state, rather than initial state, effect). We also note a recent study suggesting that trapped metal adatoms on Au(111) can affect the appearance of TPP molecules in STM.[13]

Alternatively, many studies instead focus on the interaction of the phenyl legs with the surface. For instance, a comprehensive investigation of the adsorption and conformation of a variety of tetraphenyl porphyrins (TPPs) by Brede et al.[14] on Cu(111), Cu(100), and Au(111) surfaces led to the conclusion that the identity of the metallic center of a metalloporphyrin does not affect the adsorption geometry. Instead, the adsorption site, geometry, and molecular conformation were determined by the attractive interaction of the phenyl legs and the (steric) repulsion of the pyrrole units at the core of the molecule, with the underlying substrate. A later report[15] also suggested that molecule−substrate interactions induced bending in the porphyrin core leading to a subtle interplay between the "leg" geometry and the core distortion. This coupling of the "leg" and "core" geometries is repeatedly reported as a commonly observed feature of functionalized porphryin adsorption.[11,14−17] The observed independence of the metallic center on the adsorption geometry is particularly important, as this suggests that chemical interactions between the core nitrogen atoms and the surface are insignificant, as might be expected in the case where the nitrogen atoms are already coordinated to a metal center. We also note at this point that in a previous report examining Co-metalated Br_4TPP molecules on Cu(111) Iancu et al.[16] observe two molecular conformers extremely similar in appearance to what we describe below for the free base molecule.

Despite the extensive body of theoretical and experimental studies, there are relatively few *ab initio* investigations aimed at modeling TPP adsorption incorporating dispersion corrections (see, for example, Rojas et al.[17]). The Tkatchenko group has shown, using a variety of dispersion-corrected DFT approaches, that benzene adsorption on metals has a critical dependence on vdW interactions.[18,19] Much larger molecules such as diindoperylene have also been examined where the attractive components of adsorption were found to depend almost entirely on vdW interactions.[20] The calculated dependence was so great that the adsorption energy was modified by more than 5 eV on Cu(111). It was also noted that vdW interactions on Cu(111) are significantly higher than for the other coinage metals studied and almost twice that on Au(111).

An unanswered question arising from the research on porphyrin adsorption to date therefore relates to the extent to which the combined effects of vdW interactions and the precise adsorption site controls the conformation of TPP molecules. Although many of the previous studies cited above have carefully examined the interrelationship of adsorption and molecular conformation, to date an exact assignment of the adsorption sites of porphyrin conformers relative to the atomic structure of the Cu(111) surface, along with detailed simulations of the structures observed by STM, has not been made.

Here we examine Br_4TPP using a combination of atomic and submolecular resolution STM with both DFT with dispersion and classical molecular dynamics (MD) calculations to determine the relationship between the precise adsorption geometry of Br_4TPP on Cu(111) and its conformation. Experimental measurements are carried out at low temperatures providing greater stability and reducing the possibility of potential temperature-driven effects at higher temperatures. By making a direct comparison between the experimentally determined adsorption position and the complete geometry calculated with DFT with dispersion we unambiguously determine the adsorption structure of each conformer. Furthermore, our results are supported by simulated STM images which are compared with the experimental appearance of the Br_4TPP molecules in each conformation. We show that controlled, and purely mechanical, translation of a Br_4TPP molecule from one adsorption site to another at low temperatures (5 K) results in switching between conformers via an intermediate conformational "hybrid". Moreover, MD and DFT with dispersion calculations reveal a critical dependence on vdW forces and an absence of significant chemical interaction, which is, surprisingly and perhaps counterintuitively, found to significantly modify the molecular energy levels (density of states, DOS).

The paper is structured as follows. In the first section, experimental scanning probe data are presented revealing the experimental adsorption site of each molecular conformer and the steps observed during conformational switching. In the second section, we describe MD and DFT simulations which identify the complete adsorption geometry of each conformational structure and show simulated STM images that can be compared with experiment. We then discuss the adsorption behavior of Br_4TPP, where we find strong evidence for a purely

DOI: 10.1021/acs.jpcc.5b08350
J. Phys. Chem. C XXXX, XXX, XXX−XXX

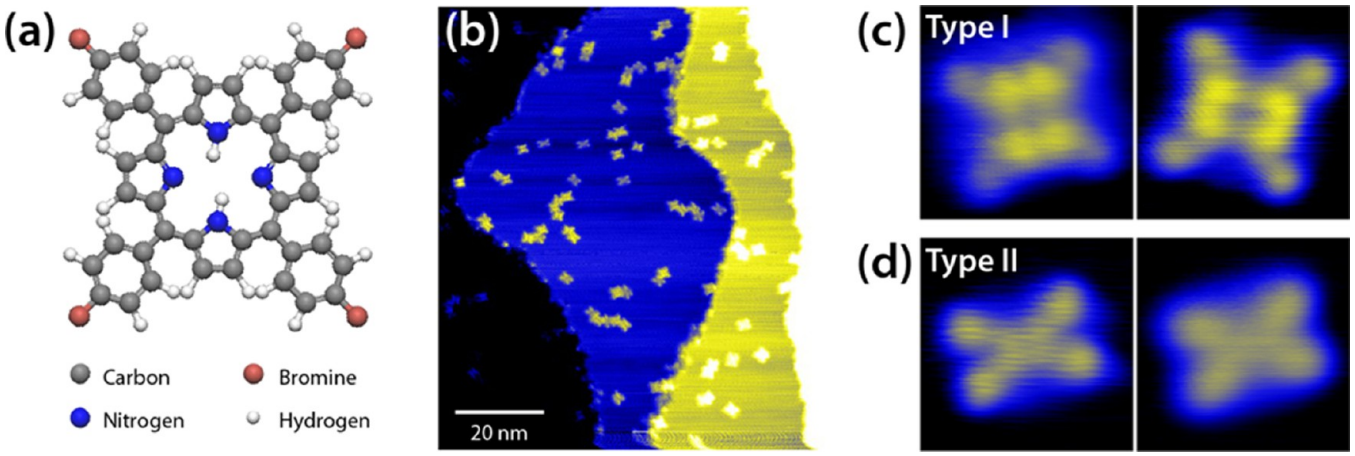

Figure 1. Typical constant current images of Br_4TPP conformers on Cu(111). (a) Planar schematic of the Br_4TPP molecule. (b) Overview image showing representative molecular coverage across four terraces of the Cu(111) surface. Note that on the largest terrace the scale is set to highlight that the molecules appear with two distinct contrast levels. Typical high-resolution images of (c) Type I conformers and (d) Type II conformers with different tip terminations. STM parameters: +1 V/50 pA. T = 77 K.

physisorbed interaction, with no evidence for chemical bond formation. In the final section, we show that such physisorbed behavior is capable of driving significant shifts in the DOS of the molecule, which can be rationalized in the context of distortion of the molecular structure and induced dipole interactions.

METHODS

Scanning Probe Microscopy. Measurements were taken on a Createc GmbH LT STM-AFM system operating under ultrahigh vacuum conditions (base pressure $<6 \times 10^{-11}$ mbar) cooled to either 77 or 5 K. A clean Cu(111) surface was initially produced by sputtering a single-crystal sample with Ne (at 800 eV; gas pressure 5×10^{-6} mbar) followed by annealing at ∼650 °C at a pressure of $\leq 5 \times 10^{-10}$ mbar. The sample was then gradually cooled to room temperature at a rate of 2 °C per second. Br_4TPP molecules were deposited using a homemade resistively heated crucible, which was heated to an estimated temperature of ∼350 ± 50 °C. The Cu(111) sample was cooled to 77 K and then placed above the crucible for 10 s at a distance of 3 cm, before being transferred to the measurement chamber.

A commercial qPlus sensor (Createc GmbH) with a tungsten tip attached to one tine of the tuning fork was used for both the STM and AFM experiments ($f_0 \sim 20$ kHz; $Q \sim 30\,000$ at 5 K; nominal spring constant 1800 N m^{-1}). Tips were electrochemically etched and introduced into the scan head without any further *ex situ* treatment. The tip was prepared *in situ* during STM imaging using controlled tip crashes and bias voltage pulsing until atomic resolution was acquired in STM feedback. As a result of this preparation process, the tips are very likely to be copper, rather than tungsten, terminated. In all measurements the bias was applied to the sample (except for the controlled molecular manipulation events, where the bias voltage was zero) and the tip held at virtual ground at the input to the preamplifier.

Electronic Structure Theory Modeling. Density functional theory calculations (DFT) were performed using the generalized gradient approximation (GGA) parametrization by Perdew—Burke—Ernzerhof (PBE)[21] implemented within the projector-augmented wave method[22,23] in the VASP software package.[24−26] The VASP plane-wave basis set energy cutoff was 400 eV, and a Gaussian smearing of 0.1 eV was used for the initial electronic occupations. To account for the missing dispersion forces in the standard implementation of DFT, we describe the vdW forces using three approaches in conjunction with the PBE exchange-correlation functional: the semi-empirical corrections proposed by Grimme (PBE-D3),[27] and the Tkatchenko−Scheffler (PBE-TS),[28] as well as the van der Waals density functional method with optimized exchange term (optB86b-vdWDF).[29]

To calculate the Cu bulk structure, a (14 × 14 × 14) Monkhorst−Pack[30] k-point mesh was used, and the resulting lattice constant for Cu was found to be 3.593/3.591/3.605 Å for the PBE-D3/PBE-TS/optB86b-vdwDF methods, respectively, all in good agreement with the experimental lattice constant of 3.610 Å. To model the surface structure, a 12 × 12 hexagonal three-layer-thick slab of Cu(111) was used. The resulting Cu(111) surface model contains in total 432 Cu atoms. The Br_4TPP ($H_{22}C_{44}N_4Br_4$) molecule was placed parallel to the surface, and a thick vacuum level of 20.0 Å was set up to ensure that there was no spurious interaction between periodically repeated slabs in the direction normal to the surface.

Geometry optimization of the Br_4TPP/Cu(111) system was performed with the Brillouin zone sampling at the Γ-point. The first two layers of the surface and the molecule are fully relaxed until the force acting on each atom is less than 0.05 eV/Å, whereas the bottom surface layer was kept fixed in the bulk position. To check the effect of the fixed bottom layer on the adsorption geometry, the constraints on the bottom layer were removed, and the further optimization was carried out relaxing all atoms in the cell. No differences were found in the calculated properties when all three layers of the Cu(111) were allowed to relax. On top of the optimized system, the single-point calculations with the (2 × 2 × 1) k-point mesh were performed, but these calculations brought negligible difference from those using the Γ-point. The density of states has been analyzed using p4vasp,[31] whereas the charge density difference and electron localization functions were visualized using VESTA.[32]

Molecular Dynamics. The Cu(111) surface slab was cut from the Cu bulk crystal, and its geometry was optimized using VASP electronic structure calculations as described above. The

DOI: 10.1021/acs.jpcc.5b08350
J. Phys. Chem. C XXXX, XXX, XXX−XXX

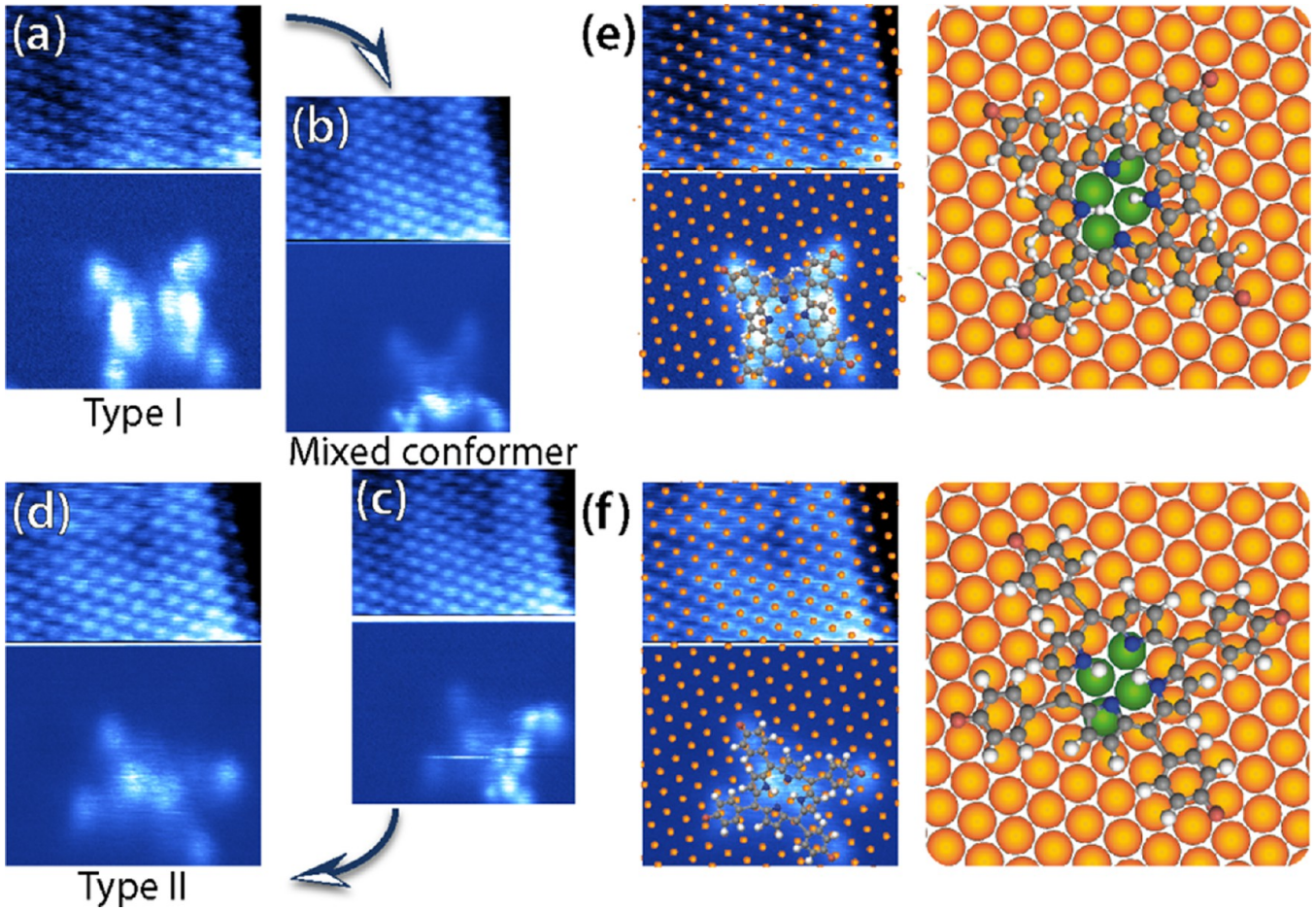

Figure 2. Sequence of constant height images of a single Br_4TPP molecule and the surrounding Cu(111) surface. (a) The Br_4TPP molecule when imaged in the initial Type I configuration. (b,c) A mixed (Type II upper-half, Type I lower-half) conformation observed after manipulation of the same molecule in (a) with the STM tip. (d) The same molecule, now imaged in the Type II conformation following further tip-induced manipulation. Superimposed structures for the Cu(111) surface and Br_4TPP molecules are shown in (e) and (f), respectively, with some copper atoms highlighted green to aid visualization. Note that the assignment of N and N−H groups is unknown from the experimental data alone. Scan parameters: 50 mV, oscillation amplitude = 300 pm; Cu(111) image height = −520 pm relative to the height used to image Br_4TPP. T = 5 K.

porphyrin molecule was placed on the surface, and a variety of molecular positions were generated over ten nanoseconds of room-temperature molecular dynamics. We used an artificially softened Cu van der Waals potential in this initial simulation, by quartering the force constant of the potential[33,34] to ensure that a wide variety of conformations were sampled within the few-nanosecond time scale of the simulation. Planar, half-saddle, and saddle conformations were identified by monitoring the elevation of the C═C carbon atoms in the core. Four starting planar conformations, four saddle conformations (two bent along the N−H−H−N direction and two bent along the N−N direction), and four half-saddle conformations (two with one bent pyrrole moiety and two with one bent deprotonated pyrrole) were extracted. The full Cu van der Waals potential was then switched on, and the 12 complexes were each subjected to a further ten nanoseconds of dynamics.

Force-field parameters for the Br_4TPP molecules were generated from existing force-field data for pyrrole[36] and 1-bromobenzene.[35] We used Gaussian09[37] electronic structure calculations to generate atomic charges for deprotonated pyrrole, 2,3-dimethyl-pyrrole, and 1-bromo-4-methyl-benzene and then mapped the natural population analysis (NPA) charge differences relative to pyrrole and 1-bromobenzene to parametrize the full porphyrin molecule. The structure generated gave negligible penalties in the CGenFF program,[38] and the charge distributions are similar in overall topology to Bader charges[39] calculated in the VASP calculations, but with lower magnitudes on the atom-centered charges.[40]

Time- and structure-averaged values for molecule conformations, dynamics, and surface adsorption energies were calculated by sampling every 20 ps over 10 ns of dynamics, to provide 200 statistically independent structures for each complex. Image generation and Tcl script-based trajectory analysis was performed using the VMD program.[41]

RESULTS

Adsorption Site Identification and Molecular Manipulation Using STM. A schematic of the tetrabromophenyl-porphyrin (Br_4TPP) molecule is shown in Figure 1(a). The molecule comprises a free-base porphyrin core terminated with four flexible brominated phenyl groups. In Figure 1(b) we show a large area STM scan of the Cu(111) surface following deposition of a submonolayer (∼10−20%) coverage of the Br_4TPP molecule at a substrate temperature of 77 K, thus preventing metalation of the porphyrin core (see Methods). Similar to previous observations,[14−16] we find that the molecules appear with two distinct types of contrast and shape, as shown in Figure 1(c) and (d). We note that

DOI: 10.1021/acs.jpcc.5b08350
J. Phys. Chem. C XXXX, XXX, XXX−XXX

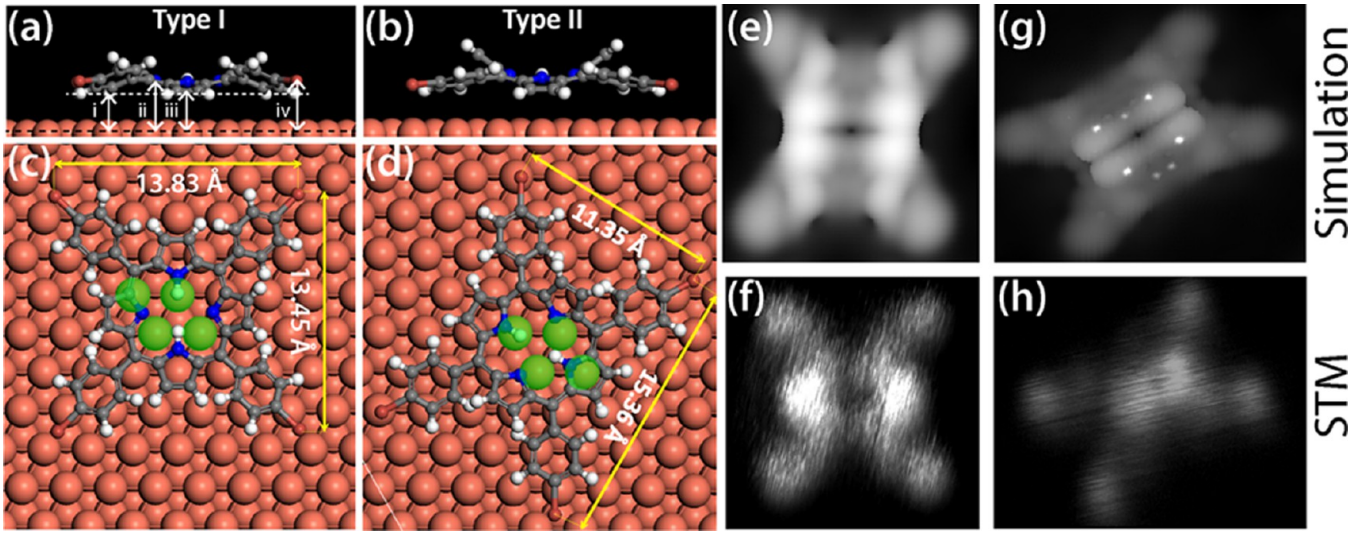

Figure 3. Stable adsorption configurations and simulated STM of Br_4TPP on Cu(111) resulting from DFT with dispersion calculations. Side-on views of the structures matching the Type I and II conformations are shown in (a) and (b), respectively, both of which adopt saddle conformations. Ball-and-stick models showing the aspect ratio and exact alignment of the Type I and II conformers with the surface are shown in (c) and (d), respectively. Copper atoms are once again highlighted green to show the exact match with the experimental structures from Figure 2. Simulated STM images are shown with their experimental counterparts for (e,f) the Type I and (g,h) the Type II conformers.

deposition of similar molecules on Cu(111) carried out with elevated substrate temperatures results in coverages consisting of only a single conformer found to adopt a saddle arrangement.[42] Two properties of the images can be used to distinguish the molecular types. Type I (Figure 1(c)) is observed with a square aspect ratio, where the core typically appears brighter compared to the "legs". Type II (Figure 1(d)) has an asymmetric aspect ratio with one axis a factor of ∼1.4 longer than the other. Additionally, the Type II molecule appears darker (under the same imaging conditions) compared to Type I, measuring topographic heights of 1.8 and 2.5 Å, respectively. This effect is particularly pronounced for the positive sample biases used throughout this study.

Deposition was carried out onto a cold substrate in order to obtain isolated single molecules where a statistical analysis across multiple experiments revealed equal proportions of each molecular conformer (see Figure S1). To ascertain the precise adsorption site of Br_4TPP on the Cu(111) surface and to gain further insights into the different appearances of the Type I and Type II molecules, we acquired STM images in constant height mode (also at 5 K) using two different z-heights. This allows us to image the molecule and the surrounding surface[43,44] *within the same scan* (and, importantly, with precisely the same tip state). We then overlay the atomic positions of the underlying Cu substrate onto the molecule as shown in Figure 2. By doing so we have found that both Type I and II conformers are orientated along the surface close-packed direction resulting in an even distribution of molecules rotated 60° with respect to one another (see Figure S1). As discussed in detail below, we find very good agreement between the adsorption site determined experimentally via this method and that predicted by not only density functional theory but also molecular dynamics simulations.

To compare the Type I and II contrast we imaged a single molecule that was controllably switched between conformations at 5 K temperatures (see Figure S2 for full sequence) using tip-induced molecular manipulation carried out at zero applied sample bias[45] (i.e., with no detectable tunnelling current that might otherwise locally heat the molecule). The scanning and the molecular manipulation in Figure 2 were carried out with an oscillation of 300 pm applied to the qPlus sensor allowing simultaneous STM and AFM imaging,[46] although no AFM data are presented in this work. The lower half of the image in Figure 2(a) shows a molecule in the Type I conformation, with the atoms of the Cu(111) surface—taken at a reduced tip−sample separation of $\Delta z \sim -520$ pm—observed in the upper half of the image. By overlaying the Cu(111) lattice onto the molecule, as in Figure 2(e), we can determine its exact adsorption site. We then laterally manipulated the molecule (Figure S2) and switched it from the Type I to the Type II conformation.

Lateral manipulation was carried out by reducing the tip height by 500 pm and laterally moving the tip across the molecule between scans. The molecules were then observed to either laterally translate, rotate, or switch conformation. Switching was most commonly observed from the Type I to the Type II conformation, suggesting that the Type II arrangement is more stable. (In work published elsewhere[47] we show that this is due to a significant increase in the energy barriers for movement of the Type II conformer across the surface, which is reflected by an increase in the lateral force required to move the molecule relative to the Type I arrangement.) Attempts to reverse the switching (i.e., to switch from Type II to Type I), although possible, were generally unsuccessful and often resulted in damage to the molecule or a change in the tip state. Consequently, the conformational "switch" we observe is not routinely reversible.

As shown in Figure 2(b) and (c), the switching process occurs via a metastable intermediate state where half of the molecule first switches to the Type II conformation before finally reaching an all-Type-II state (see Figure 2(d)), observed during a subsequent scan (Figure S2(f)). The series of images in Figure S2 exhibits a high degree of consistency in the observed adsorption position for each conformer. As such we are able to determine the exact adsorption site as shown in Figure 2(e) and (f) for the Type I and II conformers,

DOI: 10.1021/acs.jpcc.5b08350
J. Phys. Chem. C XXXX, XXX, XXX−XXX

respectively. On the basis of these observations, and the simulations discussed below, we suggest that it is the adsorption site of the molecule that determines its conformation and that the conformation can be modified by manipulating the molecule to an alternative adsorption site.

The ability to switch the conformation of the molecule between Type I and Type II by lateral manipulation across the surface is a clear indication that the position of the Br_4TPP molecule with respect to the underlying Cu(111) lattice plays a key role in determining which of the conformers is adopted. Additionally, the observation that the molecules can not only be reversibly mechanically switched at 5 K temperatures but also that one-half of the molecule is observed to switch before the other appear to suggest that metal complexes[10] are not necessarily involved in determining the conformation on Cu(111). The switching behavior especially excludes any possibility of complete metalation. The DFT and molecular dynamics results described in the following section strongly support this interpretation and highlight the essential role that vdW forces play in the conformational changes we observe.

Structure Determination via Density Functional Theory and Molecular Dynamics. In order to calculate the full adsorption geometry of each conformer we simulated the complete molecule−surface system using classical MD in addition to extensive DFT calculations incorporating several methods to account for dispersion (see SI and Methods). Due to the high flexibility of the molecule and the relatively flat potential energy surface (PES)[47] a large number of adsorption geometries were identified as stable through DFT and MD simulations, the latter identifying as many as 12 arrangements (see Figure S3), demonstrating conformations with either planar or saddle-shaped cores. The experimentally superimposed structures in Figure 2 were therefore essential in reducing the large parameter space in our calculations and were used to help guide the simulated structures (although some exploration was also conducted in order to confirm these were indeed the lowest energy structures). From this comparison, and with guidance from the MD simulations, two stable adsorption configurations were identified with DFT matching the experimental data for Br_4TPP on Cu(111), resulting from different orientations of the molecule with respect to the underlying Cu(111) lattice. The geometries as calculated using optB86b-vdWDF are shown in Figure 3. In order to make a comparison with the experimental structure we compared three primary features: (1) The alignment of the nitrogen atoms with the underlying Cu(111); (2) the aspect ratio of the molecule; and (3) the overall orientation of the molecule as compared to the surface close-packed crystal direction. On the basis of these criteria we found that the geometries shown in Figure 3(a,c) and (b,d) match best with the Type I and II overlays shown in Figure 2, respectively. The adsorption energies of the two conformers were calculated as −4.33 and −4.15 eV for the Type I and II conformers, respectively, and were of the order of hundreds of meV more stable than the alternative structures which demonstrated poorer agreement based on the criteria outlined above. That is, the structures best matching the experimental data in Figure 2 correspond to the lowest energy structures found. In addition to the optB86b-vdWDF functional, calculations were also carried out using the dispersion-corrected PBE-D3 and PBE-TS methods (see Methods section) resulting in almost identical structures and similar relative adsorption energies. It is important to note that due to the shallow PES of the system many of the alternatively calculated metastable structures show only small deviations in the exact adsorption location on Cu(111), thus making precise determination of the correct adsorption geometry exceptionally challenging without the experimental data in Figure 2. We note that when dispersion interactions were omitted from our simulations the molecular structures for both conformers (using the starting geometries shown in Figure 3) converged to a single planar structure with a reduced adsorption energy of only ∼95 meV (see Supporting Information, Figure S4), deviating from the geometries best matching our experimental results, highlighting the important role of vdW interactions in modeling both conformers.

The DFT-calculated geometries reveal important details regarding the mechanisms behind molecular adsorption. Hitherto, the conformational differences of isolated molecules on Cu(111) have been explained as due to planar and saddle orientations with respect to the surface.[16] While planar structures were observed to be stable in some of our simulations, saddle structures predominate and ultimately provided the best match with the experimental data and the lowest calculated total energies. Consequently, both of the lowest energy geometries we identify are found to significantly distort the molecule from the gas-phase structure (see SI for more details), each adopting a saddle conformation on the surface as shown in Figure 3(a) and (b). The strongest alignment of the molecules with the underlying Cu(111) substrate is observed for the phenyl and pyrrole groups, which appear to dominate the molecular adsorption. In the Type I geometry (Figure 3(c)) each of the phenyl leg groups is found to occupy positions located directly above the bridge sites of the Cu(111) in addition to three out of the four pyrrole groups. Conversely, in the Type II geometry (Figure 3(d)) the phenyl legs and three of the pyrrole groups occupy positions located above the hollow sites of the surface. This alignment stems from a strong preference for the phenyl groups to align themselves with the surface in such a way as to maximize the vdW interaction with the copper. Therefore, although vdW interactions are often considered small (of the order of a few meV per atom pair), the cumulative interaction of the 48 atoms making up the pyrrole and phenyl groups of the Br_4TPP with the Cu surface atoms is easily capable of leading to several eV in total adsorption energy. For the Type II geometry in particular, we note that the increased amount of core distortion of the molecule incurs an energy penalty. However, due to the increased tilt of the pyrrole groups the phenyl legs are able to "swing" into a more favorable position, reducing steric repulsion and increasing their interaction with the underlying copper leading to similar adsorption energies for the Type I and Type II binding arrangements and a much greater diffusion barrier.[47]

In Table 1 we list the closest molecule−surface distances of each element as depicted in Figure 3(a) alongside the corresponding covalent and vdW radii. In most cases the atomic distances are either in line with the combined vdW radii or greater. The only instance where the atomic separation falls below the vdW radii by a significant margin (yet remaining well above the covalent radii) is for the C−Cu separations and the Br−Cu distance in the Type II conformation. Such reductions in binding distance are reminiscent of hydrogen bonding; however, as described below, no permanent dipoles are present in our system. Although our calculations show that the Br−Cu interaction plays a much greater role for the Type II conformation, its effect is insufficient to compensate the high

DOI: 10.1021/acs.jpcc.5b08350
J. Phys. Chem. C XXXX, XXX, XXX−XXX

Table 1. Bond Distances as Depicted in Figure 3(a) Shown with Corresponding Covalent (r_{cov}) and vdW (r_{vdW}) Radii in Å Taken from Reference 48

		Type I	Type II	covalent radii (Å)	vdW radii (Å)
i	Cu−H	2.57	2.53	$r^{H}_{cov} + r^{Cu}_{cov} = 0.37 + 1.28 = 1.65$	$r^{H}_{vdW} + r^{Cu}_{vdW} = 1.20 + 1.40 = 2.60$
ii	Cu−N	3.34	3.51	$r^{N}_{cov} + r^{Cu}_{cov} = 0.75 + 1.28 = 2.03$	$r^{N}_{vdW} + r^{Cu}_{vdW} = 1.55 + 1.40 = 2.95$
iii	Cu−C	2.70	2.74	$r^{C}_{cov} + r^{Cu}_{cov} = 0.76 + 1.28 = 2.04$	$r^{C}_{vdW} + r^{Cu}_{vdW} = 1.80 + 1.40 = 3.20$
iv	Cu−Br	3.28	2.85	$r^{Br}_{cov} + r^{Cu}_{cov} = 1.14 + 1.28 = 2.42$	$r^{Br}_{vdW} + r^{Cu}_{vdW} = 1.85 + 1.40 = 3.25$

energy penalty from the increased distortion of the core macrocycle. This is supported by our calculations with vdW corrections removed where the molecule is always observed to relax back to a configuration close to the gas-phase structure.

To test the possibility that displaced copper atoms from the top surface layer affect the molecule−surface bonds (as proposed by Doyle et al.[10]), we modeled an adsorption configuration where the surface copper atoms located below iminic nitrogens, in addition to those closest to the surface carbon atoms and Br groups, were displaced upward by 1 Å toward the molecule to a distance well within the covalent radii. The geometry optimization was then performed where the final optimized structure simply relaxed back to the Type II configuration described above, where no copper displacements are found. This indicates that molecular "anchorage" on the surface via coordination with displaced copper atoms is somewhat unlikely at the low temperatures considered in this study, as supported by the experimental observation of the intermediate conformer and the manipulation at 5 K described above.

Simulated STM. As described above, the Type I and II conformers of Br_4TPP appear with very distinct contrasts in STM images. As such, we calculated constant current STM images for each of the conformers at a sample bias voltage of +1 V. A comparison between the simulated and experimental STM images is shown in Figure 3(e,f) and 3(g,h) for the Type I and

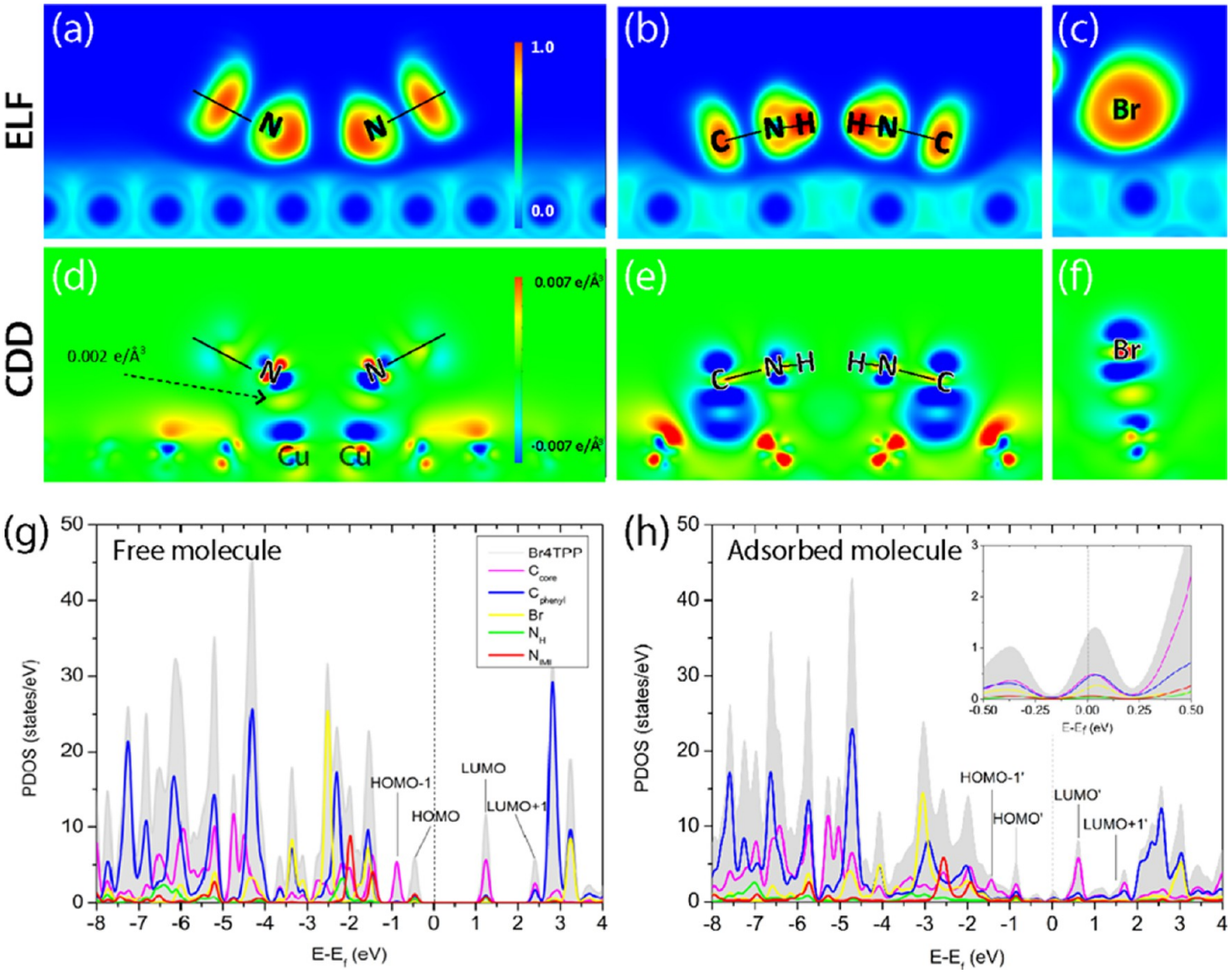

Figure 4. Determining the interaction of Br_4TPP on Cu(111). Electron localization function (ELF) and charge density difference (CDD) plotted as a 2D slice through (a),(d) the iminic nitrogen atoms, (b),(e) pyrrolic nitrogen atoms, and (c),(f) bromine terminations. ELF plots show the complete absence of chemical bonding, supported by an extremely small accumulation of charge between the N_{imi}, N_H, and Br atoms and copper surface shown in the CDD. Projected density of states (PDOS) of the free (g) and adsorbed (h) molecule where interface states (inset) are found to primarily originate from C_{core} and C_{phenyl} contributions, rather than the N_{imi} atoms.

DOI: 10.1021/acs.jpcc.5b08350
J. Phys. Chem. C XXXX, XXX, XXX−XXX

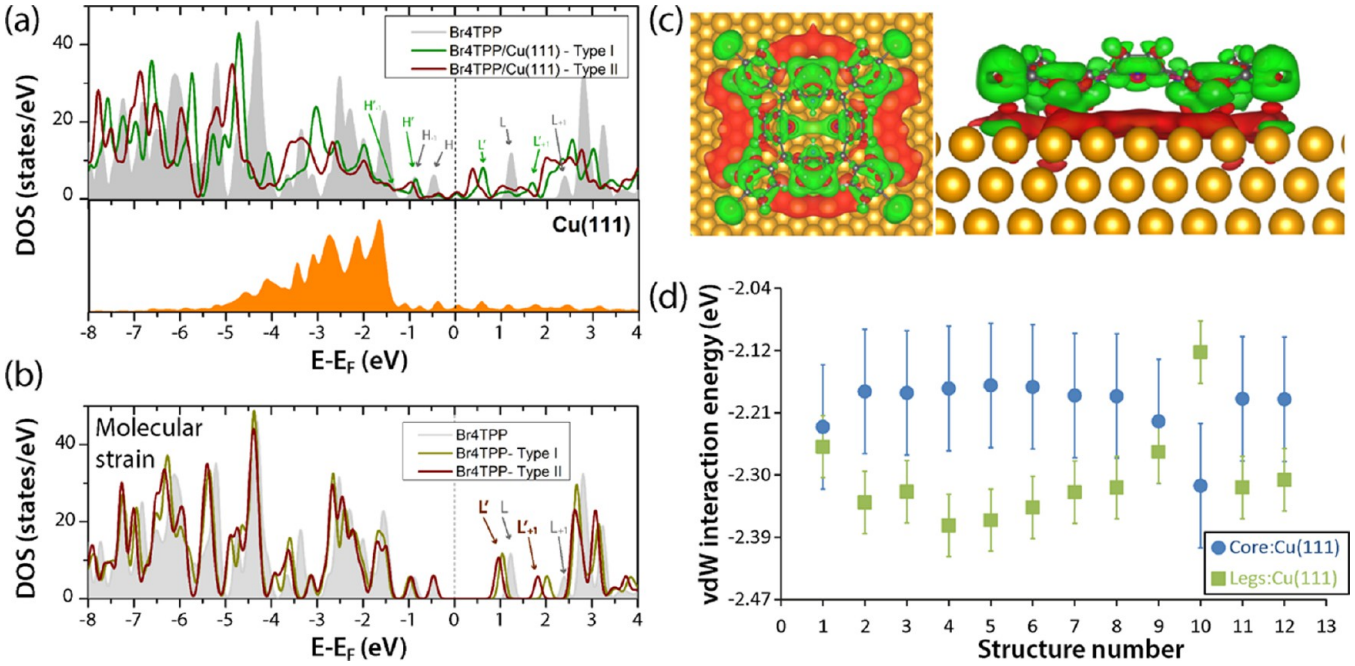

Figure 5. Physisorption-induced changes in DOS. (a) Calculated DOS for the gas-phase structure (gray), the Type I (green) and Type II (red) structures shown in Figure 3, and the Cu(111) surface (all shown relative to the copper Fermi level). The major HOMO−LUMO peaks for the gas-phase and Type I molecule are marked with arrows. (b) Calculated DOS for the Br_4TPP molecule in the gas phase (gray) as in (a) but now shown with the DOS calculated for the isolated Br_4TPP molecule with its geometry fixed in each conformation but with the Cu(111) surface removed, i.e., the change in DOS due to the modified geometry of each conformer. Significant shifts are observed for the LUMO peaks despite the complete absence of the surface. (c) Charge density difference (CDD) plotted for the Type I conformer showing the distinctive "pillow effect" caused by physisorbed behavior. Red (green) corresponds to charge accumulation (depletion) plotted with an isovalue of ±0.02 e/Å. (d) Core and leg adsorption energies extracted from molecular dynamics simulations of Br_4TPP adsorbed on Cu(111) (structure numbers relate to geometries shown in Figure S3).

II conformers, respectively. In addition to reproducing the correct appearance of the four brominated leg groups at each corner of the molecule, we find extremely good agreement for the core structure of each conformer, closely matching the two bright lobes typically observed in experiment. The experimental images shown in Figure 3 were taken in the constant height mode, which shows better detail of the molecular structure than the constant current images in Figure 1. In addition, we also find very good agreement for the aspect ratio for each conformer, which is measured as 1 and 1.35 from the ball-and-stick structure and ∼1.1 and ∼1.45 from the simulated STM, compared to experimental values of ∼1.0(1) and ∼1.4(1), for the Type I and II conformers, respectively.

As we describe in detail below, the excellent agreement we observe is due not only to determining the correct adsorption position of each conformer but also to significant changes to the electronic structure caused by the large vdW interaction the molecules have with the underlying Cu(111) surface. Therefore, based on the strong agreement we observe for both the STM images and the adsorption site, we can accurately assign the adsorption geometry of Br_4TPP on Cu(111) in each conformation.

vdW Forces Dominate Adsorption. Similar to previous studies of large planar molecules,[20] our calculations reveal that vdW forces dominate molecular adsorption. In good agreement with the DFT results, our MD calculations reveal a subtle interplay between surface adsorption (of the molecular core and phenyl legs) and the induced strain from the saddle geometry. Isolated contributions from the core and legs shown in Figure 5(d) (corresponding to the MD structures in Figure S3) illustrate how the core and leg adsorption energies compensate for one another; i.e., as the core adsorption energy improves the legs are penalized and *vice versa*. The calculated structures and energies show that overall improvements in adsorption of the molecule as a whole compensate for geometrical strain in the core, as leg groups rotate into the space underneath bent pyrrole groups to maximize the vdW interaction with the surface. The ball-and-stick structures in Figure S3 show the predominant saddle structure observed in the simulations, in which the pendant bromo-phenyl groups tilt to obtain a close vdW contact between the phenyl rings and the Cu(111) surface as described above. Control simulations of legless porphyrin molecules with just the core macrocycle showed always 100% planar structures.

To check for the presence of chemical bonding we have examined in detail the electronic structure of each conformer computing the electron localization function (ELF), charge density difference (CDD), and projected density of states (PDOS) at various sites across the molecule. As can be seen in Figure 4 neither the (a,d) iminic nitrogen atoms, (b,e) pyrrolic nitrogen atoms, nor (c,f) bromine terminations show any significant chemical interaction with the copper in either the ELF or CDD plots. The 2D CDD plots in particular show that the majority of the charge redistribution is a direct result of the "pillow effect" discussed below and visualized in Figure 5(c). In Figure 4(d) we primarily observe charge depletion between the iminic nitrogen/bromine atoms and the copper substrate, with only a very small region of excess charge, which is nonetheless over an order of magnitude smaller than what is expected for chemical bond formation in both covalent systems[43,50] and N−

DOI: 10.1021/acs.jpcc.5b08350
J. Phys. Chem. C XXXX, XXX, XXX−XXX

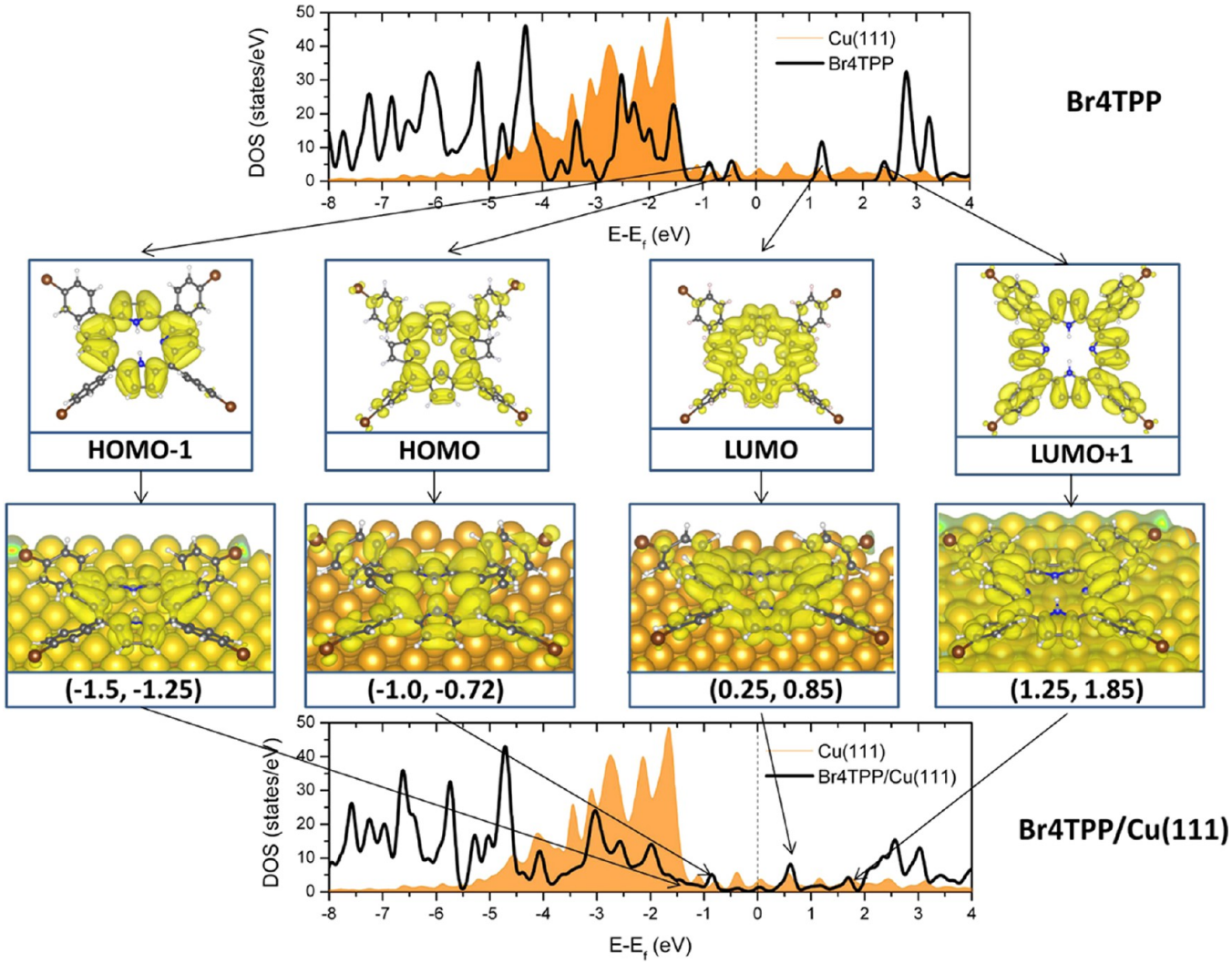

Figure 6. Integrated local density of state (ILDOS) analysis of Br_4TPP on Cu(111). (a) Calculated density of states (DOS) for the isolated gas-phase molecule and the Cu(111) surface. (b) Square modulus plots of the HOMO−1, HOMO, LUMO, and LUMO+1 orbitals for the gas-phase molecule as marked with arrows. (c) ILDOS plots showing the corresponding orbitals of the surface-adsorbed molecule. (d) Calculated DOS for the surface-adsorbed molecule and the isolated Cu(111) surface. The location of the ILDOS plots from (c) are shown with arrows.

Cu bond formation,[51] suggesting only a very weak presence of chemical bonding between the molecule and the surface.

In addition to the charge visualizations, the density of states projected onto the C_{core}, C_{phenyl}, Br, N_H, and N_{imi} atoms was calculated for both the free (Figure 4(g)) and adsorbed (Figure 4(h)) molecule. In Figure 4(h) in particular it is clearly observable that the interface states formed within the HOMO−LUMO gap originate from the carbons of the core macrocycle and the legs as well as the bromine atoms, with no contribution from the nitrogen units, an effect assigned to hybrid interface states of the weakly interacting molecule.[52,53] Critically, however, the PDOS analysis demonstrates that there is no mixing, and therefore no strong interaction, between the nitrogen atoms of the molecule and the copper. A Bader charge analysis also reveals that only a small amount of charge transfer occurs from the Cu(111) to the molecule of 0.1e and 0.07e for the Type I and II conformers, respectively, suggesting a relatively small contribution of ionic binding compared to the dominant vdW interaction.

As described above, the adopted saddle structure of the molecule significantly increases the vdW binding energy with the surface. This rearrangement results in significant charge redistribution around the phenyl leg groups and core pyrrole units, which are able to move closer to the Cu(111) surface. Additional, but more localized, vdW contributions are also observed, associated with the bromine terminations and the iminic nitrogen atoms (which are tilted toward the Cu substrate). If the dispersion is not included and the stable geometries shown in Figure 3 are allowed to relax using standard DFT, the adsorption energy drops to ∼95 meV resulting in a planar structure. Furthermore, if the molecular geometry is instead fixed in place, and the dispersion "switched off", the non-vdW adsorption energy takes on a positive value, suggesting that steric repulsion between the molecule and the surface makes up the primary contribution. We stress this final point, as it has been previously observed that the reduced molecule−surface separation induced by vdW forces can aid the onset of chemical interactions,[54] evidenced by strong localized hybridization visible in plots of the CDD. That our CDD plots show no such interaction, in addition to the drastically weakened binding we observe when dispersion corrections

DOI: 10.1021/acs.jpcc.5b08350
J. Phys. Chem. C XXXX, XXX, XXX−XXX

are "switched off" (both with fixed and relaxed geometries), however, suggests that this is not the case in our simulations.

Our investigation into the question of the physisorbed vs chemisorbed state of Br_4TPP on Cu(111) can therefore be summarized as follows. Examination of the DOS spectra for each conformer shows that the LUMO remains above the Fermi level with minimal charge transfer of 0.1e at most to the molecule. This is supported by plots of the PDOS which show negligible mixing between the nitrogen units of the molecule and the copper. In addition, a direct visualization of the charge distribution through ELF and CDD analysis reveals a lack of electronic density sufficient for chemical bonding and instead points to the dominating repulsive interaction from exchange effects (as substantiated by the positive adsorption energies calculated when dispersion corrections are removed).

We therefore conclude that the adsorption of Br_4TPP, and likely many other TPP derivatives, depends on the cumulative vdW contributions originating from both the phenyl leg groups and the core macrocycle of the molecule. It is only due to this strong interdependence between saddle conformations and improved alignment with the copper substrate that we are able to obtain the experimentally observed structures. One reason why chemical interactions may be suppressed in this system is the electron-withdrawing nature of the Br atoms, which may cause a reduction in the ionization potential of the molecule by "draining" charge from the central macrocycle, similar to other systems.[49] Additionally, it may be the case that in some experiments deprotonation of the N−H occurs leading to strongly binding N radicals. This could potentially result from irradiation during photoemission measurements or catalytic scission of the bond during annealing.

Physisorption-Induced Changes in DOS. In Figure 5(a) we compare the calculated DOS for the gas-phase structure of Br_4TPP and the two conformations it adopts on the Cu(111) surface. As shown in the Supporting Information (Figure S4), in the calculations without dispersion we observe very little change to the DOS, observing only a small shift toward positive energies. The resultant non-vdW structures were found to deviate from the two saddle arrangements best matching our experimental results to an almost single planar structure matching neither conformer. This is despite the fact that the vdW optimized structures shown in Figure 3 were used as the starting geometries in the non-vdW calculation. Remarkably, however, when dispersion forces are taken into account we observe a much larger deviation in the DOS from that calculated in the gas phase as shown in Figure 5(a). In addition to a clear broadening of the peaks we also calculate a significant shift toward more negative energy values. The maximum of the peaks that correspond to the LUMO+1/LUMO and HOMO/HOMO−1 of the free molecule are located around +1.6/0.5 and −0.9/−1.5 relative to the Cu(111) surface Fermi level. The HOMO/LUMO peaks are also easily identified by visualizing the integrated local density of states of the individual peaks before and after adsorption, as shown in Figure 6. It is important to note, however, that despite the large shifts in DOS the LUMO peak does not cross the Fermi level. Integrated local density of states (ILDOS) plots following adsorption also appear very similar to the square modulus of the isolated orbitals of the free molecule showing that the occupied (unoccupied) states in the free molecule are consistently under (above) the Fermi level. This indicates that molecular charge donation, back-donation that could be responsible for formation of the chemical bond, is marginal. We also note that the DOS plots have little or no dependence on the choice of method to describe dispersion (see Figure S5). The DOS for the isolated Br_4TPP and Cu(111) systems with and without dispersion was also calculated, as shown in Figure S6. In this case, however, the dispersion has very little effect. Consequently, the variations in DOS we observe must arise from the coupled surface−molecule system.

In the gas-phase structure of Br_4TPP the HOMO−LUMO gap is found to span a large energy window of ∼1.1 eV around the Cu(111) Fermi level (where STM imaging is typically performed). Following adsorption on the surface the LUMO peak is shifted by ∼0.8 eV. This has particularly significant implications for STM imaging, as the number of available states at positive energies near E_f is significantly increased. It therefore seems likely that the vdW-induced changes in DOS we observe are essential for obtaining the simulated STM images shown in Figure 3. Interestingly, the observed shifts differ for each of the two molecular arrangements, highlighting the important effect of conformation on the DOS. As explained below, this is likely due to a combination of the increased strain in the Type II arrangement and the difference in wave function overlap with the surface.

We suggest that the origin for the observed shifts in DOS can be understood within the context of *both* distortion of the molecular structure—thus modifying the chemical environment of its constituent parts—and induced dipole interactions caused by a significant reorganization of charge within the molecule, originating from orthogonalization of the metal and molecular wave functions.

The effect of molecular strain is shown in Figure 5(b), where the calculated DOS of the gas-phase (gray) molecule is compared to the DOS calculated for the isolated Br_4TPP conformers in each adsorbed geometry, i.e., the same fixed geometric structure as shown in Figure 3(a−d), but with the copper surface atoms completely removed. This eliminates any possibility of a surface interaction. As can be seen in Figure 5(b), this distortion of the molecule is enough by itself to drive surprisingly large changes to the chemical environment of the molecule, causing shifts in the DOS, particularly for the LUMO/LUMO+1 peaks as highlighted in the figure. This is similar to previous observations where changes in molecular geometry were observed to affect the electronic structure.[55,56] This simple calculation demonstrates that although chemisorption almost always leads to shifts in the DOS of a molecule the opposite cannot be assumed; shifts in the DOS spectrum need not arise solely from chemical bonding. This may be particularly important in the interpretation of XPS measurements, where changes in the chemical environment of atomic elements (and the associated chemical shifts in photoemission spectra) are almost always interpreted in terms of chemisorption.

The second effect causing changes in the DOS potentially originates from the so-called "pillow effect",[58] an exchange interaction driven by Pauli repulsion that causes a large reorganization of charge within the molecule. Similar to previous calculations,[17,57] we observe depletion of charge from the molecule as charge density is pushed away into the surface, shown in the charge density difference (CDD) plot in Figure 5(c). This results in a significant surface interface dipole, a common observation for physisorbed atoms and molecules.[59] Such exchange interactions have been shown to cause significant shifts in the energy levels of graphene when it is either physisorbed or chemisorbed[60] and to underpin work

DOI: 10.1021/acs.jpcc.5b08350
J. Phys. Chem. C XXXX, XXX, XXX−XXX

function changes due to Xe and cyclohexane adsorption.[59] We note that our calculations reveal only a small amount of charge transfer to the molecule of ∼0.1e, indicating a small contribution from ionic binding and supporting that the observed interface dipole likely arises from the "pillow effect".

Although vdW interactions have previously been shown to affect the HOMO/LUMO structure of a molecule,[54,57] these systems are unlikely purely physisorbed. Indeed, one case[54] reports a synergistic effect of vdW interactions in combination with chemisorption. The results described in this study show that large changes to the molecular DOS can arise from an essentially physisorbed molecule. We therefore propose that physisorption, particularly in the case of large, flexible molecules, could potentially play a significant role in inducing large changes in DOS, a behavior typically attributed to chemisorption.

CONCLUSIONS

In summary, direct comparison of low-temperature STM measurements with DFT including the effect of dispersion and classical MD have allowed us to identify the complete adsorption geometry of the two conformers adopted by Br_4TPP on Cu(111). Through combined STM imaging of each conformer with the surrounding Cu(111) surface we identify the exact experimental adsorption site. Moreover, scanning probe-driven and purely mechanical (0 V bias), low-temperature molecular manipulation demonstrates that the Br_4TPP conformers can be mechanically switched and manipulated at 5 K temperatures via an intermediate conformational state. On the basis of a comprehensive analysis of molecular geometries calculated by DFT with dispersion and classical MD we determine that vdW forces dominate molecular adsorption based on the alignment of the pyrrole and phenyl groups with the underlying Cu(111) substrate. From a comparison between experimental and calculated adsorption positions and STM images, we can assign the correct adsorption geometry of Br_4TPP on Cu(111) with a high degree of confidence. Surprisingly, we reveal that physisorption is capable of driving significant shifts in the molecular DOS. It is likely that our results have implications for a variety of molecular systems other than porphyrins, as there are many large flexible molecules known to adopt multiple conformations at surfaces.

ASSOCIATED CONTENT

Supporting Information

The Supporting Information is available free of charge on the ACS Publications website at DOI: 10.1021/acs.jpcc.5b08350.

Additional experimental results for Br_4TPP manipulation and the full simulation procedures (PDF)

AUTHOR INFORMATION

Corresponding Author

*E-mail: samuel.jarvis@nottingham.ac.uk.

Notes

The authors declare no competing financial interest.

ACKNOWLEDGMENTS

S.P.J. would like to thank the Engineering and Physical Sciences Research Council (EPSRC) and The Leverhulme Trust for the award of fellowships EP/J500483/1 and ECF-2015-005, respectively. P.M. thanks the Engineering and Physical Sciences Research Council (EPSRC) and the Leverhulme Trust, respectively, for Grants No. EP/G007837/1 and F00/114 BI. J.D.B. thanks EPSRC for grant No. EP/K016288/1 and EP/L000202. D.T. thanks Science Foundation Ireland (SFI) for financial support under Grant Number 11/SIRG/B2111 and the SFI/Higher Education Authority Irish Center for High-End Computing (ICHEC) for computing time. J.A.L. thanks for financial support from VR, Carl Tryggers Stiftelsen, and Kempestiftelserna and computational resources provided by the Swedish National Infrastructure for Computing (SNIC) at HPC2N, NSC, and PDC. N.R.C. gratefully acknowledges receipt of a Royal Society Wolfson Merit Award. A.S. thanks the German Research Foundation (DFG) for financial support under grant number SA 2625/1-1 and acknowledges financial support from the European Project ARTIST.

REFERENCES

(1) Scheidt, W. R. Explorations in Metalloporphyrin Stereochemistry, Physical Properties and Beyond. *J. Porphyrins Phthalocyanines* **2008**, *12*, 979.

(2) Senge, M. New Trends in Photobiology: The Conformational Flexibility of Tetrapyrroles − Current Model Studies and Photobiological Relevance. *J. Photochem. Photobiol., B* **1992**, *16*, 3.

(3) Stepien, M.; Sprutta, N.; Latos-Grazynski, L. Figure Eights, Mobius Bands, and More: Conformation and Aromaticity of Porphyrinoids. *Angew. Chem., Int. Ed.* **2011**, *50*, 4288.

(4) Schweitzer-Stenner, R. Using Spectroscopic Tools to Probe Porphyrin Deformation and Porphyrin-Protein Interactions. *J. Porphyrins Phthalocyanines* **2011**, *15*, 312.

(5) Scott, A. Discovering Nature's Diverse Pathways to Vitamin B12: A 35-Year Odyssey. *J. Org. Chem.* **2003**, *68*, 2529.

(6) Fleming, I. Absolute Configuration and the Structure of Chlorophyll. *Nature* **1967**, *216*, 151.

(7) Auwarter, W.; Ecija, D.; Klappenberger, F.; Barth, J. V. Porphyrins at Interfaces. *Nat. Chem.* **2015**, *7*, 105.

(8) Buchner, F.; Xiao, J.; Zillner, E.; Chen, M.; Rockert, M.; Ditze, S.; Stark, M.; Steinruck, H.; Gottfried, J. M.; Marbach, H. Diffusion, Rotation, and Surface Chemical Bond of Individual 2H-Tetraphenylporphyrin Molecules on Cu(111). *J. Phys. Chem. C* **2011**, *115*, 24172.

(9) Buchner, F.; Zillner, E.; Rockert, M.; Giessel, S.; Steinruck, H.; Marbach, H. Substrate-Mediated Phase Separation of Two Porphyrin Derivatives on Cu(111). *Chem. - Eur. J.* **2011**, *17*, 10226.

(10) Doyle, C. M.; Krasnikov, S. A.; Sergeeva, N. N.; Preobrajenski, A. B.; Vinogradov, N. A.; Sergeeva, Y. N.; Senge, M. O.; Cafolla, A. A. Evidence For the Formation of an Intermediate Complex in the Direct Metalation of Tetra(4-Bromophenyl)-Porphyrin on the Cu(111) Surface. *Chem. Commun.* **2011**, *47*, 12134.

(11) Diller, K.; Klappenberger, F.; Marschall, M.; Hermann, K.; Nefedov, A.; Woll, Ch.; Barth, J. V. Self-Metalation of 2H-Tetraphenylporphyrin on Cu(111): an X-ray Spectroscopy Study. *J. Chem. Phys.* **2012**, *136*, 014705.

(12) Simonov, K. A.; Vinogradov, N. A.; Vinogradov, A. S.; Generalov, A. V.; Zagrebina, E. M.; Martensson, N.; Cafolla, A. A.; Carpy, T.; Cunniffe, J. P.; Preobrajenski, A. B. Effect of Substrate Chemistry on the Bottom-Up Fabrication of Graphene Nanoribbons: Combined Core-Level Spectroscopy and STM Study. *J. Phys. Chem. C* **2014**, *118*, 12532.

(13) Mielke, J.; Hanke, F.; Peters, M. V.; Hecht, S.; Persson, M.; Grill, L. Adatoms Underneath Single Porphyrin Molecules on Au(111). *J. Am. Chem. Soc.* **2014**, *137*, 1844.

(14) Brede, J.; Linares, M.; Lensen, R.; Rowan, A. E.; Funk, M.; Broring, M.; Hoffmann, G.; Wiesendanger, R. Adsorption and Conformation of Porphyrins on Metallic Surfaces. *J. Vac. Sci. Technol. B* **2009**, *27*, 799.

(15) Brede, J.; Linares, M.; Kuck, S.; Schwobel, J.; Scarfato, A.; Chang, S.; Hoffmann, G.; Wiesendanger, R.; Lensen, R.; Kouwer, P. H.

DOI: 10.1021/acs.jpcc.5b08350
J. Phys. Chem. C XXXX, XXX, XXX−XXX

J.; et al. Dynamics of Molecular Self-Ordering in Tetraphenyl Porphyrin Monolayers on Metallic Substrates. *Nanotechnology* **2009**, *20*, 275602.
(16) Iancu, V.; Deshpande, A.; Hla, S. W. Manipulating Kondo Temperature via Single Molecule Switching. *Nano Lett.* **2006**, *6*, 820.
(17) Rojas, G.; Simpson, S.; Chen, X.; Kunkel, D. A.; Nitz, J.; Xiao, J.; Dowben, P. A.; Zurek, E.; Enders, A. Surface State Engineering of Molecule-Molecule Interactions. *Phys. Chem. Chem. Phys.* **2012**, *14*, 4971.
(18) Carrasco, J.; Liu, W.; Michaelides, A.; Tkatchenko, A. Insight into the Description of van der Waals Forces For Benzene Adsorption on Transition Metal (111) Surfaces. *J. Chem. Phys.* **2014**, *140*, 084704.
(19) Liu, W.; Filimonov, S. N.; Carrasco, J.; Tkatchenko, A. Molecular Switches From Benzene Derivatives Adsorbed on Metal Surfaces. *Nat. Commun.* **2013**, *4*, 2569.
(20) Burker, C.; Ferri, N.; Tkatchenko, A.; Gerlach, A.; Niederhausen, J.; Hosokai, T.; Duhm, S.; Zegenhagen, J.; Koch, N.; Schreiber, F. Exploring the Bonding of Large Hydrocarbons on Noble Metals: Diindoperylene on Cu(111), Ag(111), and Au(111). *Phys. Rev. B: Condens. Matter Mater. Phys.* **2013**, *87*, 165443.
(21) Perdew, J. P.; Burke, K.; Ernzerhof, M. Generalized Gradient Approximation Made Simple. *Phys. Rev. Lett.* **1996**, *77*, 3865.
(22) Blochl, P. E. Projector Augmented-Wave Method. *Phys. Rev. B: Condens. Matter Mater. Phys.* **1994**, *50*, 17953.
(23) Kresse, G.; Joubert, D. From Ultrasoft Pseudopotentials to the Projector Augmented-Wave Method. *Phys. Rev. B: Condens. Matter Mater. Phys.* **1999**, *59*, 1758.
(24) Kresse, G.; Hafner, J. Ab Initio Molecular Dynamics for Liquid Metals. *Phys. Rev. B: Condens. Matter Mater. Phys.* **1993**, *47*, 558.
(25) Kresse, G.; Hafner, J. Ab Initio Molecular-Dynamics Simulation of the Liquid-Metal-Amorphous-Semiconductor Transition in Germanium. *Phys. Rev. B: Condens. Matter Mater. Phys.* **1994**, *49*, 14251.
(26) Kresse, G.; Furthmuller, J. Efficiency of Ab-Initio Total Energy Calculations For Metals and Semiconductors Using a Plane-Wave Basis Set. *Comput. Mater. Sci.* **1996**, *6*, 15.
(27) Grimme, S. Semiempirical GGA-Type Density Functional Constructed With a Long-Range Dispersion Correction. *J. Comput. Chem.* **2006**, *27*, 1787.
(28) Tkatchenko, A.; Scheffler, M. Accurate Molecular Van Der Waals Interactions from Ground-State Electron Density and Free-Atom Reference Data. *Phys. Rev. Lett.* **2009**, *102*, 073005.
(29) Klimes, J.; Bowler, D. R.; Michaelides, A. Van Der Waals Density Functionals Applied to Solids. *Phys. Rev. B: Condens. Matter Mater. Phys.* **2011**, *83*, 195131.
(30) Monkhorst, H. J.; Pack, J. D. Special Points for Brillouin-Zone Integrations. *Phys. Rev. B* **1976**, *13*, 5188.
(31) p4vasp available from: http://www.p4vasp.at/.
(32) Momma, K.; Izumi, F. VESTA 3 for Three-Dimensional Visualization of Crystal, Volumetric and Morphology Data. *J. Appl. Crystallogr.* **2011**, *44*, 1272.
(33) Heinz, H.; Vaia, R. A.; Farmer, B. L.; Naik, R. R. Accurate Simulation of Surfaces and Interfaces of Face-Centered Cubic Metals Using 12−6 and 9−6 Lennard-Jones Potentials. *J. Phys. Chem. C* **2008**, *112*, 17281.
(34) Phillips, J. C.; Braun, R.; Wang, W.; Gumbart, J.; Tajkhorshid, E.; Villa, E.; Chipot, C.; Skeel, R. D.; Kalé, L.; Schulten, K. Scalable Molecular Dynamics With NAMD. *J. Comput. Chem.* **2005**, *26*, 1781.
(35) MacKerell, A. D.; Bashford, D.; Bellott; Dunbrack, R. L.; Evanseck, J. D.; Field, M. J.; Fischer, S.; Gao, J.; Guo, H.; Ha, S.; et al. All-Atom Empirical Potential For Molecular Modeling and Dynamics Studies of Proteins. *J. Phys. Chem. B* **1998**, *102*, 3586.
(36) Vanommeslaeghe, K.; Hatcher, E.; Acharya, C.; Kundu, S.; Zhong, S.; Shim, J.; Darian, E.; Guvench, O.; Lopes, P.; Vorobyov, I.; et al. CHARMM general force field: A force field for drug-like molecules compatible with the CHARMM all-atom additive biological force fields. *J. Comput. Chem.* **2010**, *31*, 671.
(37) Frisch, M. J.; Trucks, G. W.; Schlegel, H. B.; Scuseria, G. E.; Robb, M. A.; Cheeseman, J. R.; Scalmani, G.; Barone, V.; Mennucci, B.; Petersson, G. A. et al. *Gaussian 09*, Revision A.1; Gaussian Inc.: Wallingford CT, 2009.
(38) We use version 2b8, the latest version posted in September 2013. Program and methodology is outlined at http://mackerell.umaryland.edu/kenno/cgenff/ and in: (a) Vanommeslaeghe, K.; MacKerell, A. D., Jr. Automation of the CHARMM General Force Field (CGenFF) I: Bond Perception and Atom Typing. *J. Chem. Inf. Model.* **2012**, *52*, 3144. (b) Vanommeslaeghe, K.; Prabhu Raman, E.; MacKerell, A. D., Jr. Automation of the CHARMM General Force Field (CGenFF) II: Assignment of Bonded Parameters and Partial Atomic Charges. *J. Chem. Inf. Model.* **2012**, *52*, 3155.
(39) Henkelman, G.; Arnaldsson, A.; Jónsson, H. A Fast and Robust Algorithm For Bader Decomposition of Charge Density. *Comput. Mater. Sci.* **2006**, *36*, 354.
(40) Simulation input files and calculated porphyrin−Cu(111) structures are available on request.
(41) Humphrey, W.; Dalke, A.; Schulten, K. VMD: Visual Molecular Dynamics. *J. Mol. Graphics* **1996**, *14*, 33.
(42) Weber-Bargioni, A.; Auwarter, W.; Klappenberger, F.; Reichert, J.; Lefrancois, S.; Strunskus, T.; Woll, C.; Schiffrin, A.; Pennec, Y.; Barth, J. V. Visualizing the Frontier Orbitals of a Conformationally Adapted Metalloporphyrin. *ChemPhysChem* **2008**, *9*, 89.
(43) Chiutu, C.; Sweetman, A. M.; Lakin, A. J.; Stannard, A.; Jarvis, S.; Kantorovich, L.; Dunn, J. L.; Moriarty, P. Precise Orientation of a Single C60 Molecule on the Tip of a Scanning Probe Microscope. *Phys. Rev. Lett.* **2012**, *108*, 268302.
(44) Schuler, B.; Liu, W.; Tkatchenko, A.; Moll, N.; Meyer, G.; Mistry, A.; Fox, D.; Gross, L. Adsorption Geometry Determination of Single Molecules by Atomic Force Microscopy. *Phys. Rev. Lett.* **2013**, *111*, 106103.
(45) Custance, O.; Perez, R.; Morita, S. Atomic Force Microscopy as a Tool For Atom Manipulation. *Nat. Nanotechnol.* **2009**, *4*, 803.
(46) Sweetman, A.; Stannard, A.; Sugimoto, Y.; Abe, M.; Morita, S.; Moriarty, P. Simultaneous Noncontact AFM and STM of Ag:Si(111)-($\sqrt{3}\times\sqrt{3}$)R30. *Phys. Rev. B: Condens. Matter Mater. Phys.* **2013**, *87*, 075310.
(47) Jarvis, S. P.; Taylor, S.; Baran, J. D.; Champness, N. R.; Larsson, J. A.; Moriarty, P. Measuring the Mechanical Properties of Molecular Conformers. *Nat. Commun.* **2015**, *6*, 8338.
(48) Bondi, A. Van Der Waals Volumes and Radii. *J. Phys. Chem.* **1964**, *68*, 441. Sutton, L. E. *Table of Interatomic Distances and Configuration in Molecules and Ions*, Supplement 1956−1959, Special publication No. 18, Chemical Society: London, UK, 1965.
(49) Baran, J. D.; Gronbeck, H.; Hellman, A. Analysis of Porphyrines as Catalysts for Electrochemical Reduction of O_2 and Oxidation of H_2O. *J. Am. Chem. Soc.* **2014**, *136*, 1320.
(50) Schwarz, A.; Gao, D. Z.; Lammle, K.; Grenz, J.; Watkins, M. B.; Shluger, A. L.; Wiesendanger, R. Determining Adsorption Geometry, Bonding, and Translational Pathways of a Metal-Organic Complex on an Oxide Surface: Co-Salen on NiO(001). *J. Phys. Chem. C* **2013**, *117*, 1105.
(51) Kovačević, N.; Kokalj, A. DFT Study of Interaction of Azoles with Cu(111) and Al(111) Surfaces: Role of Azole Nitrogen Atoms and Dipole-Dipole Interactions. *J. Phys. Chem. C* **2011**, *115*, 24189.
(52) Caplins, B.; Suich, D. E.; Shearer, A. J.; Harris, C. B. Metal/Phthalocyanine Hybrid Interface States on Ag(111). *J. Phys. Chem. Lett.* **2014**, *5*, 1679.
(53) Temirov, R.; Soubatch, S.; Luican, A.; Tautz, F. S. Free-Electron-Like Dispersion in an Organic Monolayer Film on a Metal Substrate. *Nature* **2006**, *444*, 350.
(54) Liu, W.; Carrasco, J.; Santra, B.; Michaelides, A.; Scheffler, M.; Tkatchenko, A. Benzene Adsorbed on Metals: Concerted Effect of Covalency and Van Der Waals Bonding. *Phys. Rev. B: Condens. Matter Mater. Phys.* **2012**, *86*, 245405.
(55) Qiu, X. H.; Nazin, G. V.; Ho, W. Mechanisms of Reversible Conformational Transitions in a Single Molecule. *Phys. Rev. Lett.* **2004**, *93*, 196806−1.
(56) Auwarter, W.; Seufert, K.; Klappenberger, F.; Reichert, J.; Weber-Bargioni, A.; Verdini, A.; Cvetko, D.; Dell'Angela, M.;

DOI: 10.1021/acs.jpcc.5b08350
J. Phys. Chem. C XXXX, XXX, XXX−XXX

Floreano, L.; Cossaro, A.; et al. Site-Specific Electronic and Geometric Interface Structure of Co-Tetraphenyl-Porphyrin Layers on Ag(111). *Phys. Rev. B: Condens. Matter Mater. Phys.* **2010**, *81*, 245403.
(57) Chilukuri, B.; Mazur, U.; Hipps, K. W. Effect of Dispersion on Surface Interactions of Cobalt(II) Octaethylporphyrin Monolayer on Au(111) and HOPG(0001) Substrates: a Comparative First Principles Study. *Phys. Chem. Chem. Phys.* **2014**, *16*, 14096.
(58) Vázquez, H.; Dappe, Y. J.; Ortega, J.; Flores, F. A Unified Model For Metal/Organic Interfaces: IDIS, 'Pillow' Effect and Molecular Permanent Dipoles. *Appl. Surf. Sci.* **2007**, *254*, 378.
(59) Bagus, P.; Staemmler, V.; Woll, C. Exchangelike Effects for Closed-Shell Adsorbates: Interface Dipole and Work Function. *Phys. Rev. Lett.* **2002**, *89*, 096104.
(60) Gong, C.; Lee, G.; Shan, B.; Vogel, E. M.; Wallace, R. M.; Cho, K. First-Principles Study of Metal-Graphene Interfaces. *J. Appl. Phys.* **2010**, *108*, 123711.

DOI: 10.1021/acs.jpcc.5b08350
J. Phys. Chem. C XXXX, XXX, XXX−XXX